# Evolution of the Pseudogap State of High-$T_c$ Superconductors with Doping

A. V. Puchkov,[1] P. Fournier,[2,3] D. N. Basov,[1] T. Timusk,[1] A. Kapitulnik,[2] and N. N. Kolesnikov[4]

[1]*Department of Physics and Astronomy, McMaster University, Hamilton, Ontario, Canada L8S4M1*
[2]*Edward L. Ginzton Laboratory, Stanford University, Stanford, California 94305*
[3]*Center for Superconductivity Research and Department of Physics, University of Maryland, College Park, Maryland 20742*
[4]*Institute of Solid State Physics, Chernogolovka, Russia, 142432*

We report on a study of the infrared properties of $Bi_2Sr_2CaCu_2O_{8+\delta}$, $Bi_{1.66}Pb_{0.34}Sr_2CaCu_2O_{8+\delta}$, and $Tl_2Ba_2CuO_{6+\delta}$ crystals at doping levels from underdoped to strongly overdoped. We calculate the frequency-dependent scattering rate $1/\tau(\omega, T)$ and study its doping dependence. While we observe a normal-state gaplike depression in $1/\tau(\omega, T)$ in the underdoped regime, it is not observed in the overdoped regime. While the high-frequency $1/\tau(\omega, T)$ is temperature independent in the underdoped regime, it scales with temperature in the overdoped regime. [S0031-9007(96)01373-7]

The doping phase diagram of high-$T_c$ superconducting (HTSC) materials can be divided into three regions: (i) underdoped, where the superconducting transition temperature $T_c$ increases with increased hole doping; (ii) optimally doped, where $T_c$ reaches its maximum; (iii) overdoped, where a material becomes a better metal as the hole doping progresses but $T_c$ is decreasing.

It is well established that the normal-state transport properties of HTSC are profoundly different from those of conventional metals. This includes the linear-$T$ dc resistivity at the near-to-optimal doping level [1–3], along with the temperature-dependent Hall coefficient [3,4] and the unusual shape and temperature dependence of the complex optical conductivity $\sigma(\omega) = \sigma_1(\omega) + i\sigma_2(\omega)$ [5]. The unconventional normal-state transport properties are usually viewed as a manifestation of the strongly correlated nature of the charge dynamics in HTSC. Previous optical measurements on underdoped $YBa_2Cu_3O_{7-\delta}$ (Y123) and $YBa_2Cu_4O_8$ (Y124) systems revealed evidence for a gap formation in the spectrum of electronic excitations at $T > T_c$ [6–8] (since the gap is not complete, it is usually referred to as a pseudogap). In this Letter we extend these results and examine evolution of the charge dynamics in HTSC as a function of doping, for the first time performing systematic measurements in the whole doping range from underdoped to strongly overdoped.

The shape of $\sigma_1(\omega)$ of a simple metal is normally well accounted for by the Drude formula that describes the free-carrier contribution to $\sigma_1(\omega)$ as a Lorentzian peak centered at zero frequency with an oscillator strength $\omega_p^2/8$ and a width determined by a frequency-independent scattering rate $1/\tau$ [5,9]. However, the Drude formula is strictly applicable for simple metals at low frequencies and low temperature where elastic scattering from impurities and weak quasielastic scattering from thermally excited excitations such as phonons dominate [5,10]. In the case of a strongly interacting electronic system the optical properties can be described by making the damping term

frequency dependent. This formalisms, usually referred to as the extended Drude model, were developed to describe the infrared conductivity of metals with a strong electron-phonon interaction and proved to be extremely successful for such materials such as Pb [11]. It has been applied to the HTSC cuprates as well [8,12].

One starts by rewriting the complex conductivity $\sigma(\omega)$ in terms of a complex damping function, also called a memory function, $G(\omega) = 1/\tau(\omega) - i\omega\lambda(\omega)$ [5],

$$\sigma(\omega) = \sigma_1(\omega) + i\sigma_2(\omega) = \frac{\omega_p^2/4\pi}{G(\omega) - i\omega}. \quad (1)$$

The quantities $1/\tau(\omega)$ and $\lambda(\omega)$ describe the frequency-dependent (unrenormalized) carrier scattering rate and mass enhancement so that the effective mass is given by $m^*(\omega) = m_{bare}[1 + \lambda(\omega)]$. The $1/\tau(\omega)$ and $\lambda(\omega)$ can be found from the experimentally determined complex optical conductivity $\sigma(\omega)$,

$$1/\tau(\omega) = \frac{\omega_p^2}{4\pi} \text{Re}\left(\frac{1}{\sigma(\omega)}\right),$$
$$1 + \lambda(\omega) = -\frac{\omega_p^2}{4\pi\omega} \text{Im}\left(\frac{1}{\sigma(\omega)}\right), \quad (2)$$

where $\omega_p$ is a plasma frequency of the charge carriers that can be found from the sum rule $\int_0^\infty \sigma_1(\omega)\,d\omega = \omega_p^2/8$. The $\lambda(\omega)$ and $1/\tau(\omega)$ obey Kramers-Kronig relations [5].

Using the above approach, we demonstrate dramatically different charge dynamics on the two opposite ends of the phase diagram. Consistent with the previous work on the underdoped Y123 system [6–8], our experimental results in the underdoped region show a pseudogap in $1/\tau(\omega, T)$ at $T < 140-160$ K and frequencies below $\sim 700$ cm$^{-1}$. For the first time we extend these measurements to the overdoped regime where we do not observe the pseudogap. Furthermore, while the high-frequency part of $1/\tau(\omega, T)$ is linear and surprisingly temperature independent in the underdoped regime, it becomes temperature dependent and superlinear as doping is increased to near and above optimal levels.

       

To determine $1/\tau(\omega, T)$ we performed reflectivity measurements on two underdoped and one overdoped $Bi_2Sr_2CaCu_2O_{8+\delta}$ (Bi2212), on overdoped $Bi_{1.66}Pb_{0.34}Sr_2CaCu_2O_{8+\delta}$ [(Bi/Pb)2212], and on two overdoped $Tl_2Ba_2CuO_{6+\delta}$ (Tl2201) single crystals. The details of crystal growth are reported elsewhere [13]. The measurements were performed in a broad energy range $30-40\,000$ cm$^{-1}$. We calculate the real and imaginary parts of the optical conductivity using Kramers-Kronig relations, and $1/\tau(\omega, T)$ using Eqs. (1) and (2).

The experimentally obtained real part of the optical conductivity $\sigma_1(\omega)$ for Bi2212 is plotted in the upper panels of Fig. 1 at doping levels from significantly underdoped to slightly overdoped. As in other cuprates already at room temperature $\sigma_1(\omega)$ is not Lorentzian, which one would expect for a simple metal. As the temperature is reduced from 300 K the conductivity changes shape with spectral weight redistributing to form a narrow peak at low frequencies at the expense of the higher frequency region. This makes the shape of $\sigma_1(\omega)$, with its rapid frequency dependence at low frequencies followed by an almost frequency-independent $\sigma_1(\omega)$, even more unusual. This behavior is especially prominent in the underdoped samples. As the temperature is reduced below $T_c$ a part of the spectral weight shifts to a $\delta$ peak at zero frequency, which represents the superconducting response. This reduces the spectral weight located at finite frequencies by an amount proportional to a density of superconducting carriers. The difference between the optical conductivity curves obtained at temperatures just above $T_c$ and well below $T_c$ is the largest in the slightly overdoped sample, while in the most underdoped sample it is very small.

To pinpoint the changes in the shape of the optical conductivity we have plotted the frequency-dependent scattering rate of Eqs. (2) in the lower panels. Starting with the underdoped material with $T_c = 0.73 T_c^{\max} = 67$ K we find that the room temperature $1/\tau(\omega)$ is linear in the en-

ergy region up to at least 3000 cm$^{-1}$ [14], with a small upward deviation from linearity below 700 cm$^{-1}$ [15]. As the temperature decreases, the high-frequency part of $1/\tau(\omega, T)$ does not change, while below 700 cm$^{-1}$ the scattering rate $1/\tau(\omega, T)$ is depressed forming a sharp pseudogap structure. The reduction of $1/\tau(\omega, T)$ corresponds to the biasing of the spectral weight of $\sigma_1(\omega)$ towards low energies as the charge carriers experience less scattering. The dots on the vertical axis represent $1/\tau_{dc}(T)$ obtained from dc resistivity measurements [2,16]. A fair agreement with the extrapolated optical values is observed. We note that the requirement of continuity between the metallic $1/\tau_{dc}(T)$ and the temperature-independent high-frequency $1/\tau(\omega, T)$ inevitably implies the existence of the pseudogap. One can say that the metallic dc resistivity is a result of the pseudogap opening and is caused by the low-energy electron dynamics. A similar pseudogap feature has been previously observed optically in underdoped Y123 [6–8] and $YBa_2Cu_4O_8$ materials [7,8].

There is no clear understanding at this time of the mechanism that makes $1/\tau(\omega)$ linear up to at least 0.4 eV. In the conventional theory of electron-boson scattering [10,11] the low-temperature $1/\tau(\omega, T)$ is effectively an integral of the boson spectral density $A(\Omega)$ over energies from zero to $\omega$ which would imply that $A(\Omega)$ is a frequency-independent, nonzero constant over a large energy range. It was shown [10] that a quasilinear behavior can continue to energies about twice the upper cutoff energy of the bosonic spectrum, above which $A(\Omega) = 0$. Even taking this into account, the experimentally observed linearity of $1/\tau(\omega, T)$ up to 0.4 eV implies that the cutoff energy must be higher than, for example, the phonon $A(\Omega) = \alpha^2 F(\Omega)$, where $F(\Omega)$ is a phonon density of states with a cutoff at 0.1 eV [17].

The temperature independence of $1/\tau(\omega, T)$ at high frequencies for the underdoped crystals is even harder to understand. The conventional electron-boson scattering theory requires the high-energy scattering rate to increase with temperature, $1/\tau(\omega, T) \sim T$ at high enough $T$. Our experimental results for $1/\tau(\omega, T)$ for underdoped Bi2212 ($T_c = 67$ K) crystal show no sign of temperature dependence above 800 cm$^{-1}$. The only way to account for this behavior in the framework of the electron-boson scattering theory is to assume that the spectral function $A(\Omega)$ is also a function of *temperature*: $A(\Omega, T)$. In this case, if the absolute value of $A(\Omega, T)$ scales properly with temperature, it may be responsible for the observed temperature-independent scattering rate at high frequencies. However, the physical reasons for this type of behavior are not clear. Therefore, the opening of the pseudogap and the temperature-independent high-frequency $1/\tau(\omega, T)$ *both* add up to a very peculiar state of electron dynamics in underdoped Bi2212. From a completely different point of view, the two component model of optical conductivity [5], where infrared conductivity is divided into a free carrier and a midinfrared component, these observations
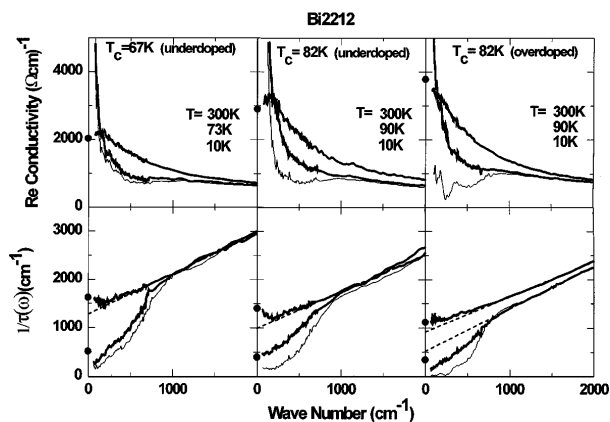


FIG. 1. The optical conductivity $\sigma_1(\omega, T)$ and scattering rate $1/\tau(\omega, T)$ for Bi2212 at several doping levels. The temperatures shown are room temperature, just above $T_c$, and well below $T_c$ (thin lines). The straight dashed lines show a linear fit to $1/\tau(\omega, T)$ over frequencies $800-3000$ cm$^{-1}$, while the dots show the results of dc measurements.

imply that the midinfrared component is temperature independent in underdoped materials.

The $1/\tau(\omega, T)$ spectra for Bi2212 at higher doping levels are shown in the remaining two lower panels of Fig. 1. As doping progresses, the absolute value of the $1/\tau(\omega, T)$ decreases slightly in agreement with the decreasing dc resistivity. The depth of the normal-state pseudogap decreases with doping as well, mainly as a result of the decreased absolute value of $1/\tau(\omega, T)$ at high frequencies. However, the position of the pseudogap, defined as the frequency where $1/\tau(\omega, T)$ deviated from the linear in $\omega$, does not change significantly with doping within our error margin. The high-frequency $1/\tau(\omega, T)$ remains essentially linear [15], with a somewhat decreased slope, even in the slightly overdoped Bi2212. As doping is increased above optimal a clear temperature dependence (however, still much slower than $k_B T$) develops.

We are not aware of theoretical work that would describe $1/\tau(\omega, T)$ in the superconducting state. However, we would like to point out that the shapes of the normal state and the superconducting state $1/\tau(\omega, T)$ are very similar in an underdoped regime. While the pseudogap that started to develop at temperatures well above $T_c$ is deepened in the superconducting state, its overall shape does not change. This suggests that at least some of the essential properties of the superconducting state develop in the normal state and that there are no further substantial changes to the electronic configuration below $T_c$.

Since the strongly overdoped regime is not accessible in Bi2212, we have chosen Tl2201 and (Bi/Pb)2212 materials to study this region. The $\sigma_1(\omega)$ and $1/\tau(\omega, T)$ spectra for Tl2201 and (Bi/Pb)2212 are shown in Fig. 2. None of these overdoped samples shows a distinct normal-state pseudogap similar to the one in underdoped Bi2212. However, as the temperature is reduced below $T_c$ a structure, very similar to the pseudogap in the *normal state* of underdoped cuprates, appears. While the scattering rate for the maximum $T_c$ Tl2201 sample ($T_c = 90$ K) is still fairly linear at all normal-state temperatures, unlike the underdoped Bi2212, and in agreement with the results on slightly overdoped Bi2212, the high-frequency $1/\tau(\omega, T)$ is now temperature dependent. As we proceed to the more overdoped (Bi/Pb)2212, the temperature dependence of the high-frequency $1/\tau(\omega, T)$ increases in magnitude. This trend intensifies in the strongly overdoped $T_c = 23$ K Tl2201, where the $1/\tau(\omega, T)$ spectra scale upwards almost parallel to each other with increasing temperature. However, in the $T_c = 23$ K Tl2201 sample the shape of $1/\tau(\omega, T)$ deviates from linear dependence, flattening out at low frequencies. Unlike the underdoped case where metallic $\rho_{\rm dc}(T)$ was exclusively due to the low-frequency electron dynamics (the pseudogap), in the strongly overdoped Tl2201 it is a result of temperature-induced changes in a much larger energy range.

We note a resemblance of the pseudogap feature in $1/\tau(\omega, T)$ to the angle-resolved photoemission spectroscopy (ARPES) results [18] obtained with the same
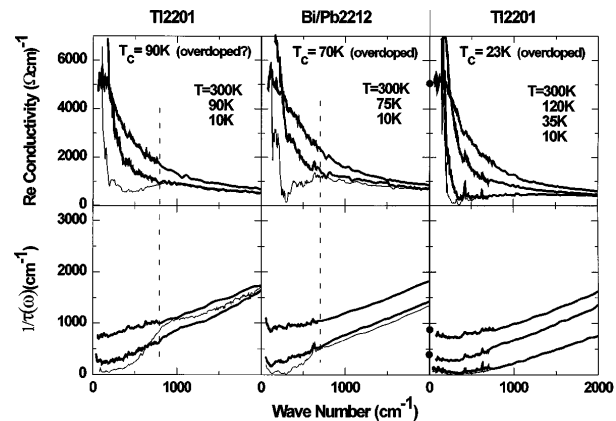


FIG. 2. The optical conductivity $\sigma_1(\omega, T)$ and scattering rate $1/\tau(\omega, T)$ for Tl2201 at doping levels with $T_c = 90$ K (maximum) and $T_c = 23$ K (strongly overdoped) and Bi/Pb2212 with $T_c = 70$ K (overdoped). The spectra at $T = 10$ K are shown by the thin lines.

batch of Bi2212 crystals. The ARPES results show an opening of a *normal-state* energy gap near $(\pi, 0)$ in *underdoped* Bi2212. Since optical measurements are not $k$ resolved, we see an average over all $k$ directions, that is, a pseudogap. As soon as the doping is increased to the overdoped regime the ARPES results show a restored large Fermi surface in agreement with the disappearance of the pseudogap in the optical $1/\tau(\omega, T)$. The remaining small pseudogap found in our measurements on the slightly overdoped Bi2212 sample may be associated with the somewhat better sensitivity of our measurements [19].

The ARPES results, in agreement with our observations, do not show much difference between the normal and the superconducting states of the underdoped Bi2212. This, along with the $d$-wave-like symmetry of the ARPES gap, led to a suggestion that the normal-state ARPES gap is a precursor of the superconducting gap. The low carrier density in the underdoped regime may result in quasiparticle pairing without pair-pair coherence at temperatures well above the actual $T_c$, producing a pseudogap [20]. As doping is increased to optimal, the carrier density increases and the effect disappears along with the normal-state pseudogap. In our experiments, the shape of $1/\tau(\omega, T)$ in the normal and the superconducting states is very similar in the strongly underdoped regime. As the doping is increased a difference develops which becomes progressively larger until no normal-state pseudogap can be observed in the overdoped samples while the superconducting $1/\tau(\omega, T)$ has the same overall shape throughout most of the doping range [in Tl2201 with $T_c = 23$ K the shape of low-frequency $1/\tau(\omega, T)$ is difficult to assess since the absolute value is too small].

Scattering of charge carriers by local antiferromagnetic (AFM) fluctuations may also contribute to the creation of the pseudogap. The energy scale associated with spin fluctuations is measured [21] to be of the order of 50 meV. The pseudogap structure that we observe

is on the same scale, supporting such models. The ARPES results also do not contradict this scenario [18]. Since the AFM fluctuations become less important as the doping increases, moving a material farther away from the antiferromagnetic order, this scattering disappears.

In summary, we observe two qualitatively different regimes of electron dynamics at opposite ends of the doping phase diagram. While in the underdoped materials the scattering rate $1/\tau(\omega, T)$ changes with $\omega$ at low frequencies much faster than the $1/\tau(\omega, T) \sim \omega$ high-frequency dependence, giving rise to a pseudogaplike depression, in the overdoped regime the low-frequency $1/\tau(\omega, T)$ changes much more slowly with $\omega$ than the high-frequency $1/\tau(\omega, T)$. Finally, while in the underdoped regime the high-frequency $1/\tau(\omega, T)$ is temperature independent; in the overdoped regime it is temperature dependent.

[1] M. Gurvitch and A.T. Fliory, Phys. Rev. Lett. **59**, 1337 (1987).
[2] C. Kendziora et al., Phys. Rev. B **48**, 3531 (1993).
[3] T. Manako et al., Phys. Rev. B **46**, 11 019 (1992).
[4] H.L. Stormer et al., Phys. Rev. B **38**, 2472 (1988).
[5] D.B. Tanner and T. Timusk, in *Physical Properties of High Temperature Superconductors III*, edited by D.M. Ginsberg (World Scientific, Singapore, 1992), pp. 363–469.
[6] J. Orenstein et al., Phys. Rev. B **42**, 6342 (1990).
[7] Z. Schlesinger et al., Physica (Amsterdam) **235-240C**, 49 (1994); L.D. Rotter et al., Phys. Rev. Lett. **67**, 2741 (1991).
[8] D.N. Basov et al. (unpublished).
[9] N.W. Ashcroft and N.D. Mermin, *Solid State Physics* (Saunders College, Philadelphia, 1976).
[10] S.V. Shulga et al., Physica (Amsterdam) **178C**, 266 (1991).
[11] P.B. Allen, Phys. Rev. B **3**, 305 (1971).
[12] G.A. Thomas et al., Phys. Rev. Lett. **61**, 1313 (1988); R.T. Collins et al., Phys. Rev. B **39**, 6571 (1989); C.T. Rieck et al., Phys. Rev. B **51**, 3772 (1995).
[13] P. Fournier et al., Physica (Amsterdam) **257C**, 291 (1996); N.N. Kolesnikov et al., Physica (Amsterdam) **242C**, 385 (1995).
[14] Equation (2) can be rewritten as $1/\tau(\omega) = \omega_p \omega \, \mathrm{Im}(1/[\epsilon(\omega) - 1])$, therefore when $\mathrm{Re}[\epsilon(\omega)] \gg 1$ the $1/\tau(\omega) \sim \omega$ behavior is related to the quadratic in $\omega$ behavior of the loss function $\mathrm{Im}[-1/\epsilon(\omega)]$, reported as a generic feature of HTSC, I. Bosovic et al., Phys. Rev. B **46**, 1182 (1992).
[15] The dashed lines in Fig. 1 represent a linear fit to $1/\tau(\omega)$ in the energy range from 800 to 3000 cm$^{-1}$.
[16] As we are not aware of published $\rho_{dc}(T)$ for overdoped Bi2212 with $T_c \simeq 82$ K, we used sum rule $\int_0^\infty [\sigma_2(\omega)/\omega]\,d\omega = \pi/(2\rho_{dc})$ to evaluate $\rho_{dc}(T)$ for this sample.
[17] B. Renker et al., Z. Phys. B **77**, 65 (1989).
[18] D.S. Marshall et al. (unpublished); A.G. Loeser et al. (unpublished).
[19] Since the ARPES leading edge in the cuprates is broad, a midpoint technique is usually employed. Although this method reproduces the doping trends well, magnitude of the gap may be ambiguous.
[20] V.J. Emery and S.A. Kivelson, Nature (London) **374**, 434 (1995).
[21] P. Bourges et al., J. Phys. Chem Solids **56**, 1937 (1995).